



ENTE PER LE NUOVE TECNOLOGIE
L'ENERGIA E L'AMBIENTE

**ELECTRICAL CONDUCTIVITY
OF ELECTROLYTIC MATRIX
FOR MOLTEN CARBONATE
FUEL CELL**

L. GIORGI, E. SIMONETTI, A. POZIO



ENTE PER LE NUOVE TECNOLOGIE
L'ENERGIA E L'AMBIENTE

ELECTRICAL CONDUCTIVITY OF ELECTROLYTIC MATRIX FOR MOLTEN CARBONATE FUEL CELL

L. GIORGI, E. SIMONETTI
ENEA - Area Energia
Centro Ricerche Energia Casaccia, Roma

A. POZIO
ENEA Guest

Testo pervenuto nel maggio 1993

I contenuti tecnico-scientifici dei rapporti tecnici dell'ENEA
rispecchiano l'opinione degli autori e non necessariamente quella dell'ente.

ABSTRACT

An overview of the electrical conductivity of molten salts and in particular of the molten alkaline carbonates is presented. The interaction of different alkali metals on the equivalent conductivity is discussed together to the migration mechanisms and salt mixtures structure.

The aim of the experimental work was to study the electrical conductivity of the electrolytic matrix used in the molten carbonate fuel cell (MCFC) and to set-up a methodology to obtain the true value for this parameter. For this purpose a laboratory scale cell was used in different experimental conditions and with electrolytic matrix having different compositions.

An analysis of the error sources in the determination of conductivity was performed and a methodology based on the electrochemical impedance spectroscopy was set-up.

The results of the measurements show that the conductivity follows an Arrhenius type equation as a function of the temperature, but the relationship is the same used for electrolytic aqueous solution. The conduction mechanism is more complicated because the molten carbonates have a mixed structure ranging from that of electrolytic solution to that of a ionic solids.

No influence of the gas composition on the conductivity values was found; that means the concentrations of oxygen species (O^{2-} , O_2^{2-} , O_2^-) is very low.

It is necessary to use high frequencies (>20 kHz) to measure the electrolytic matrix resistance, otherwise the error could be higher than 10%.

The lower activation energies are achieved with the higher carbonates/ceramic ratio in the electrolytic matrix; that was explained considering the not conductive nature of the $LiAlO_2$ ceramic and the distribution of the molten salts on its surface.

RIASSUNTO

Viene presentata la teoria della conducibilita' dei sali fusi ed in particolare dei carbonati alcalini. Segue una discussione sui meccanismi di migrazione e sulle strutture possibili dei sali fusi e l'influenza della composizione dei metalli alcalini sulla conducibilita' equivalente.

Lo scopo del lavoro sperimentale e' stato quello di studiare la conducibilita' elettrica della matrice elettrolitica impiegata nelle celle a combustibile a carbonati fusi (MCFC) e di mettere a punto una metodologia per ricavare il valore reale di tale parametro. A tale scopo e' stata impiegata una cella in scala di laboratorio operante in differenti condizioni sperimentali e con matrici elettrolitiche a differente composizione. Inoltre e' stata effettuata un'analisi delle sorgenti di errore ed e' stata messa a punto una metodologia di misura basata sulla spettroscopia di impedenza elettrochimica.

I risultati delle misure mostrano che la conducibilita' e' funzione della temperatura secondo un'equazione tipo Arrhenius usata anche per le soluzioni acquose. Nel caso dei carbonati fusi il meccanismo di conduzione e' piu' complicato in quanto questi ultimi hanno una struttura mista che possiede caratteristiche proprie sia delle soluzioni di elettroliti che dei solidi ionici.

Non e' stata trovata alcuna influenza da parte della composizione dei gas catodici sulla conducibilita' dell'elettrolita; cio' significa che la concentrazione delle specie ossidiche e' molto bassa.

Allo scopo di ridurre l'errore nella misura della resistenza della matrice elettrolitica, e' necessario utilizzare frequenze superiori a 20 kHz.

Le piu' basse energie di attivazione si ottengono con il piu' alto rapporto carbonati/ceramico nella matrice elettrolitica; cio' e' stato spiegato considerando la natura non conduttrice dell'alluminato di litio e la distribuzione dei sali fusi sulla sua superficie.

1 - INTRODUCTION

A fuel cell is a device able to generate electrical current by an electrochemical process; therefore the maximum current will depend by electrochemical and electrical characteristics of the system. The electrochemical characteristics are a function of reversible electrode potentials and electrodic reaction rates (exchange current densities); the electrical characteristics are a function of electrical conductivity of active components (electrodes and electrolyte).

The output electrical current is given by:

$$(1) \quad i = (E_a - E_c - V) / R$$

in which E_a and E_c are, respectively, the reversible anode and cathode potential at $i=0$, V the cell voltage during current output and R the sum of electrodes and electrolyte ohmic drops.

From eq.1, the current drops with an hyperbolic law as R is increased; since the electrodes conductivity is very high, it is evident that a high electrolyte conductivity is essential for a high current output by the cell.

In the case of a molten carbonate fuel cell (MCFC) , the electrolyte is constituted by molten salts, then we are in presence of a particular electrolyte both as structure and electrical properties.

The aim of the present work was to set up a methodology to measure the electrical conductivity of a ceramic-molten salts composite used in MCFC as electrolyte.

2 - ELECTRICAL CONDUCTIVITY IN MOLTEN SALTS

2.1 - Theory of ionic conductivity in molten salts

The molten salts are a class of high temperature liquid with properties ranging from those of simple ionic liquids (in the case of alkali halides) to those of liquids made by associated complexes (in the case of phosphates, borates, nitrates and carbonates) [1].

The main components of ionic molten salts are: free ions, complex ions and empty spaces. Therefore the ionic character of solid crystalline phase is present in the molten condition, also if local aggregation reactions with clusters generation could be present.

From a general point of view, the electrical conductivity of a material is given by the sum of ionic (σ_i) and electronic (σ_e) contributions:

$$(2) \quad \sigma = \sum_i \sigma_i + \sigma_e$$

In the case of purely electronic conductors (e.g. metals), σ is an inverse function of temperature, since an increase of this latter has as consequence an increase of lattice vibration and, a slow down of the free electrons motion. On the contrary, the temperature influence on ionic conductors is opposite: a temperature increase leads to a high ions mobility and, as a consequence, an increase of the conductivity.

The ions motion, in ionic solid, is due to lattice defects (vacancies and interstitial sites), while, in ionic liquid, the motion is essentially due to concentration gradients caused by structural defects.

In molten salts, in which electronic conductivity is quite negligible [2], both the gradient concentration and lattice defects mechanism are possible, but one or the other can be dominant.

Generally, a formation and motion energy is associated to each structural defect; both contribute to the total activation energy (E_{act}) for mobile ionic species.

The conductivity can be expressed as:

$$(3) \quad \sigma = \sum_i n_i \mu_i z_i e$$

where n_i , μ_i and z_i are, respectively, concentration, mobility and charge of mobile ion species.

The mobility is correlated to the diffusion coefficient following the Nernst- Einstein law:

$$(4) \quad \mu kT = zeD$$

$$(5) \quad D = \alpha \gamma^2 f_0 \exp(-E_m/kT)$$

in which α , γ , f_0 and E_m are, respectively, a parameter function of the number of dimensions in which the ion can move, the average jump distance, the vibration frequency at equilibrium position and the migration energy.

The charge carrier concentration is given by a statistical distribution as the following:

$$(6) \quad n = n_0 \exp(-E_c/kT)$$

with n_0 the total number of carriers and E_c the energy necessary to create the carriers.

Combining the equation (3) to (6), the following expression for the conductivity is obtained:

$$(7a) \quad \sigma = \sigma_0/T \exp(-E_c/kT)$$

where $\sigma_0 = n_0 z^2 e^2 \alpha \gamma^2 f_0 / k$.

The eq.7a has a general validity for condensed systems, but can also be substituted by

$$(7b) \quad \sigma = \sigma_0 \exp(-E_c/kT)$$

which is valid for glasses above the transition temperature and for electrolytic solutions.

2.2 - Electrical conductivity of molten carbonate

The molten carbonate electrical conductivity was determined by several authors [3,4,5,6] in different experimental conditions, using various types of measurement techniques.

The data obtained by Janz [3] for pure carbonates, Spedding [6] and Tanase [7] for carbonate mixtures, were correlated to temperature by means of Arrhenius plots.

The conductivity is a function of chemical composition as shown in tab. 1, in which the results obtained by several authors are summarised [8].

Tab.1 - Electrical conductivity of molten carbonate mixtures at two different temperatures, as a function of the alkali metal molar ratio.

Salts mixtures (%mol)	Electrical conductivity (S/cm)			Electrical conductivity (S/cm)		
	T = 600 °C			T = 700 °C		
Li/Na=52/48	1.83	1.75	2.00	2.50	2.42	2.55
Li/K=43/57	0.85	0.90	1.20	1.27	1.35	1.55
Li/K=50/50		0.95	1.23		1.39	1.59
Li/K=62/38		1.15	1.44		1.63	1.86
Na/K=41/59	1.17		1.26	1.53		1.59

The additivity equivalent conductivity Markov rule foresees:

$$(8a) \quad \Lambda_M = x_1^2 \Lambda_1 + x_2^2 \Lambda_2 + 2x_1 x_2 \Lambda_{12}$$

in which Λ_{12} is the equivalent conductivity of a pure component with the higher activation energy and x_i is the molar fraction of i-th component.

Ward [4] and Janz [3], in the case of carbonate mixtures, found deviation ranging from 5 to 15%; therefore, they proposed a correction to take in to account a cooperative conduction mechanism. In such a mechanism the Tobolski parameter [9] is considered:

$$(9) \quad \vartheta = (d_1 - d_2) / (d_1 + d_2)$$

with d_1 and d_2 the internuclear distances of ionic pair ($M_1^+ CO_3^{2-}$) and ($M_2^+ CO_3^{2-}$).

With such a parameter the real conductivity is:

$$(8b) \quad \Lambda_r = (1 - \vartheta) \Lambda_M$$

The d_1 and d_2 values for molten alkaline carbonate between 500 and 650 °C are not available, and as a consequence, it is not possible to use equation (8b) in the operative temperature range of mCFC.

Spedding [10] observed the Markov additivity rule which is satisfied if the mixed term in equation (8a) is generated by equivalent conductivity of the component with the smaller size cation.

A latter refinement is possible calculating again Λ_{12} from experimental data; the Λ_{12} activation energies are very similar for the three carbonate mixtures (Li/Na/K) investigated by Spedding, but that is not true for the pre-exponential terms. So, the conductivity estimation is a semiempirical measure.

Karpachev [5] measured the carbonates conductivity in a wide range of mixtures composition between 600 and 700 °C. The resulting conductivity profiles [8] for $\text{LiCO}_3\text{-Na}_2\text{CO}_3\text{-K}_2\text{CO}_3$ mixtures, are shown in fig.1.

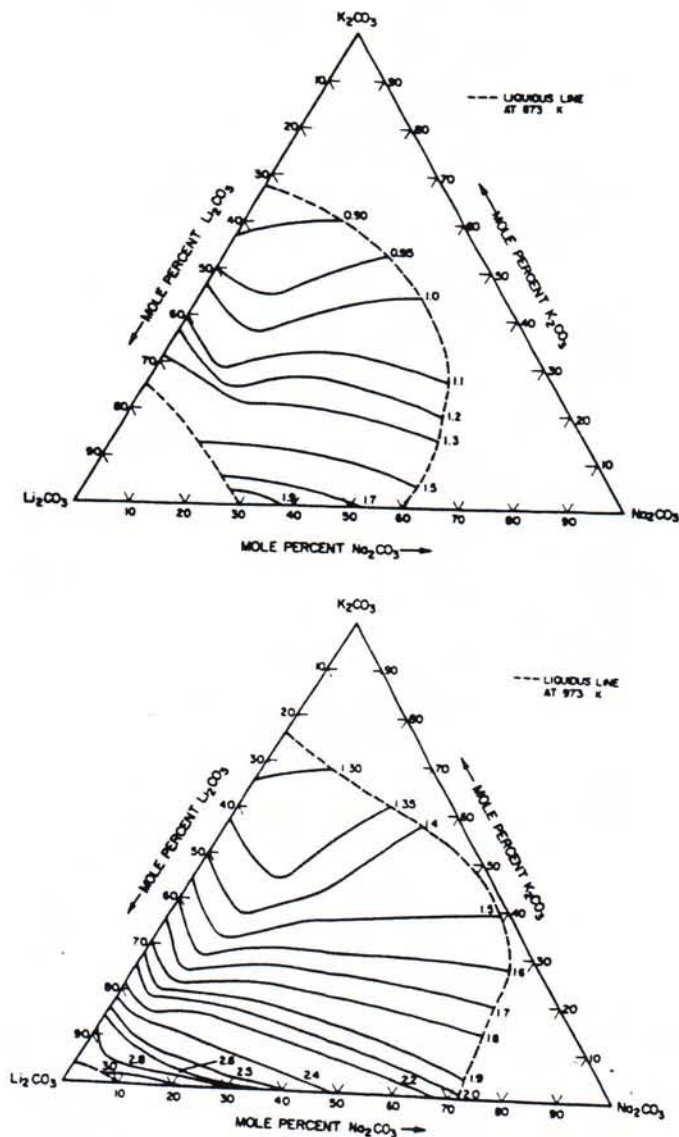


Fig.1 - Conductivity profiles for Li/Na/K carbonate mixtures, at 600 and 700°C.

From such a diagrams we point out:

- a) for a constant molar fraction of Li_2CO_3 , the conductivity near the eutectic composition increases by 10% as Na_2CO_3 increases by 9%;
- b) the addition of Na_2CO_3 to a $\text{K}_2\text{CO}_3/\text{Li}_2\text{CO}_3$ mixture (close to eutectic composition) does not increase the conductivity in a proportional way;
- c) for a constant ratio Na/K, the lithium concentration changes have a greater effect for composition close to the Li/K eutectic than the Li/K/Na eutectic.

If the specific conductivity is the only parameter to determine the MCFC operative characteristics, then a Li/Na mixture, lithium enriched, will be the optimum electrolyte.

Such an observations are also interesting for a current and potential distribution analysis. In fact, in porous electrodes concentration gradients for alkali metal ions are possible and, as result, the conductivity changes in the Li/Na/K mixtures, can be relevant.

2.3 - Electrical conductivity of ceramic/carbonate composite

The conductivity data that can be found in literature, are essentially referred to molten salts, but further to consider the electrolyte it is essential to study the ceramic/carbonate composite (electrolyte matrix or tile). In fact, in an actual MCFC, the electrolyte consists of a ceramic support ($\gamma\text{-LiAlO}_2$) filled with a salts mixture. In such a configuration, the conductivity does not depend on ceramic powder characteristics (particles dimensions and porosity), but on the volumetric fraction (p), as shown by Russell equation [9]:

$$(10) \quad \sigma_{\text{matrix}}/\sigma_{\text{electrolyte}} = (1 - p^{2/3}) / (1 - p^{2/3} + p)$$

or by Odelevskii equation [15]:

$$(11) \quad \sigma_{\text{matrix}}/\sigma_{\text{electrolyte}} = (1 - p) / (1 + 0.5p)$$

Both the equations underestimate the conductivity of electrolyte matrix by 10%.

3 - EXPERIMENTAL

3.1 - Materials and experimental conditions

A laboratory scale MCFC made of recrystallized alumina, already described [10,11], was used.

The measurements were carried out on three different tiles using two different configurations : anode / tile /cathode and cathode / tile / cathode.

The anode / tile /cathode configuration let us to perform the measurements in the real operative conditions of MCFC. The two cathodes configuration let us to avoid the contribute of the anode and reference electrodes.

Anode and cathode characteristics are summarised in tab.2.

Tab.2 - Physical-chemical characteristics of the electrodes (d_p = pore medium diameter, P = porosity, l = thickness, s = surface geometric area).

Electrode	Material	d_p (μm)	P (%)	l (mm)	s (cm^2)
cathode	NiO(Li)	8.0 ± 1.0	65 ± 5	0.38 ± 0.03	3
anode	Ni-10 Cr	9.0 ± 1.0	75 ± 5	0.76 ± 0.05	3

Tiles with different composition, but with the same preparation procedure, were used (tab. 3): alkali carbonates (Li/K=62/38 %_{mol}) mixed with γ -LiAlO₂ and hot pressed at 500°C with an applied pressure of 35 MPa.

Tab. 3 - Electrolyte matrix characteristics.

Sample	Thickness (cm)	Carbonates (% _w)	LiAlO ₂ (% _w)
A	0.18	45	55
B	0.18	45	55
C	0.15	52	48

The experimental conditions were changed for any sample (tab.4), so it was possible to evaluate their influence on the conductivity values.

Tab.4 - Experimental conditions for the investigated tiles.

Sample	Anode			Cathode		
	pH ₂ (atm)	pCO ₂ (atm)	T _{hum} (°C)	pO ₂ (atm)	pCO ₂ (atm)	T _{hum} (°C)
A	0.60	0.40	60	0.15	0.25	60
B	0.70	0.30	60	0.17	0.17	25
C	-	-	-	0.14	0.30	-

In the case of sample A and B (same composition and thickness), the hydration temperature (T_{hum}) of cathodic gases was changed to verify the influence of a strong humidified gas. For the sample C a dry gas with a composition similar to that of sample A was used.

3.2 - Measurement of electrolyte matrix electrical conductivity.

The indiscriminate use for molten salts conductivity measurement of the techniques developed for the aqueous dilute solutions, can be the cause of big mistakes. Being the molten salts highly conductive, it is easy to originate polarizations at electrodes and, as consequence, a frequency dispersion of the measurements.

The electrical conductivity σ of a liquid and its resistance R_s are related by the relation:

$$(12) \quad \sigma = d / R_s s$$

in which d/s is the cell constant, given by the ratio between the electrodes distance and their surface area.

To avoid polarisation problems it is necessary to operate with sinusoidal perturbation. The most known technique is that based on the Kolrausch bridge. It is possible to demonstrate that the measured resistance by this technique is given by:

$$(13) \quad R_m = R_s + 1/R_s C_{dl}^2 \omega^2$$

with R_s electrolyte resistance, C_{dl} electrochemical double layer capacitance and ω pulse of analysing signal.

From eq. (13) it is clear that R_m is not the true electrolyte resistance. The second term of the equation, in the case of dilute aqueous solution (high R_s values), can be neglected and therefore the R_m value gives a good estimation of R_s independently from the measurement frequency.

Since, in molten salts the R_s values are very low, the relative error can be very high. Considering a double layer capacitance of $100 \mu\text{F}/\text{cm}^2$, the measured R_m values are summarised in tab. 5, from which it is clear that the measurement frequency influences the deviation from R_s . It results that is better to operate to the higher possible frequency.

Another cause of not correct R_s values is the presence of interfacial phenomena that can be place at the electrodes. Such a phenomena are evident at low frequencies when the applied signal exceeds the minimum value necessary to activate the electrochemical processes. As consequence, the R_s value become:

$$(14) \quad R_m = R_s + 1/R_s C_{dl}^2 \omega^2 + R_f$$

in which R_f is the faradic resistance related to the electrochemical processes originate at electrode/electrolyte interface.

To reduce the influence of R_f it is necessary to use low amplitude signals and frequencies as higher as possible.

Tab. 5 - R_m calculated values as function of measurement frequency.

$R_s = 0.1 \text{ ohm/cm}^2$			
f_{meas} (Hz)	$1/\text{Re}Cdl^2\omega^2$ (ohm)	R_{meas} (ohm)	deviation (%)
1	$2.54 \cdot 10^7$	$2.54 \cdot 10^7$	$2.54 \cdot 10^{10}$
10	$2.54 \cdot 10^5$	$2.54 \cdot 10^5$	$2.54 \cdot 10^8$
10^2	$2.54 \cdot 10^3$	$2.54 \cdot 10^3$	$2.54 \cdot 10^6$
10^3	$2.54 \cdot 10^1$	$2.55 \cdot 10^1$	$2.54 \cdot 10^4$
10^4	$2.54 \cdot 10^{-1}$	$3.54 \cdot 10^{-1}$	$2.54 \cdot 10^2$
10^5	$2.54 \cdot 10^{-1}$	$1.03 \cdot 10^{-1}$	2.54

$R_s = 2 \text{ ohm/cm}^2$			
f_{meas} (Hz)	$1/\text{Re}Cdl^2\omega^2$ (ohm)	R_{meas} (ohm)	deviation (%)
1	$1.27 \cdot 10^6$	$1.27 \cdot 10^5$	$6.34 \cdot 10^7$
10	$1.27 \cdot 10^4$	$1.27 \cdot 10^3$	$6.34 \cdot 10^5$
10^2	$1.27 \cdot 10^2$	$1.29 \cdot 10^1$	$6.34 \cdot 10^3$
10^3	$1.27 \cdot 10$	3.27	$6.34 \cdot 10^1$
10^4	$1.27 \cdot 10^{-2}$	2.01	$6.34 \cdot 10^{-1}$
10^5	$1.27 \cdot 10^{-4}$	2.00	$6.34 \cdot 10^{-3}$

Due to the described problems, the tile conductivity measurements can not be carried out in direct current. During the polarisation necessary to the measure, the migration of the ions in the electrolyte could be place, with generation of dishomogeneity and electrodepletion which can change the interfacial conditions.

Following these considerations, an alternating current methodology, avoiding electrodes contribution to measure the electrolyte impedance, was used. Such a technique, different by the classic one based on the Kolrausch bridge, is the electrochemical impedance spectroscopy (EIS).

3.3 - Fundamental aspect of electrochemical impedance spectroscopy (EIS).

The EIS is a powerful technique for the study of electrochemical phenomena which take place at the electrode/electrolyte interface and for the study of electrochemical systems [13-15]. The EIS power is due to the fact that it is a steady state technique, that means it can be able to assess to phenomena with different time constant. To work in a steady state way, let us to use mediated signals for every single measurement; so it is possible to obtain the desired precision level and a large bandwidth (typically from 0,1 mHz to 1 MHz). That is possible by the use of transfer function analysers (TFA), also named frequency response analyser (FRA).

The principle of a frequency response analyser is based on the study of the system linear response to an arbitrary perturbation. Such a response can be described by a transfer function like the following:

$$(15) \quad H(s) = \{V(s)\} / \{I(s)\}$$

in which s is the Laplace frequency, $\{V(s)\}$ and $\{I(s)\}$ are the Laplace transforms of time dependent voltage and current [16].

In sinusoidal steady state terms, in the frequency domain, the transfer function become:

$$(16) \quad H(j\omega) = F\{V(t)\} / F\{I(t)\} = V(j\omega) / I(j\omega)$$

where F is the Fourier transform, ω the pulse ($2\pi f$), while $V(j\omega)$ and $I(j\omega)$ represent the sinusoidal voltage and current.

If the system is in condition of linearity, it obeys to the causality and the interface is stable during the sampling interval [17,18]. In this case the transfer function can be identifies with the impedance $Z(j\omega)$ of the system we are studying. Since $H(j\omega)$ and $Z(j\omega)$ are vectorial quantities, they are complex number containing information on both amplitude and phase angle.

From a theoretical point of view, the impedance (or more generally, the transfer function) is one of the most important measurable quantities in electrochemistry. That is because the transfer function, if sampled with an infinite bandwidth, will contain all the system information with an electrical meaning.

Since the impedance is a complex number, it is commonly written in the form:

$$(17) \quad Z(j\omega) = Z_{Re} - jZ_{Im}$$

in which Z_{Re} (real component) and Z_{Im} (imaginary component) are frequency dependent real numbers, correlated to impedance amplitude and phase angle :

$$(18) \quad Z(j\omega) = (Z_{Re}^2 + Z_{Im}^2)^{0,5}$$

$$(19) \quad \phi = \text{arctg} (-Z_{Im}/Z_{Re})$$

Impedance can be described also by the following equation:

$$(20) \quad Z(j\omega) = |Z| e^{j\phi}$$

Such a mathematical forms lead to the two graphical representations (fig.2) commonly used for the analysis of the EIS data: Nyquist plot ($-Z_{Im}$ vs. Z_{Re}) and Bode plot (ϕ and $\log |Z|$ vs $\log f$).

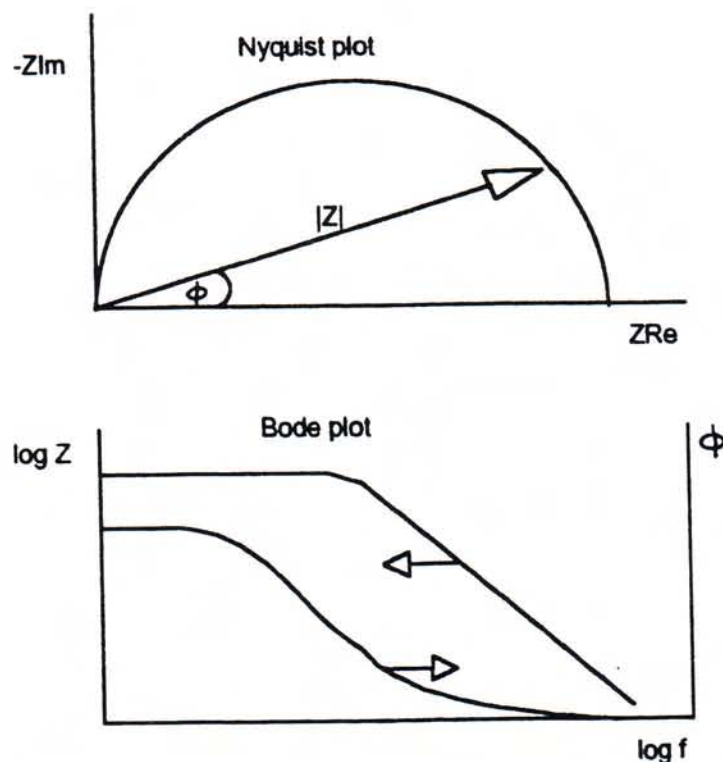


Fig.2 - Graphical representations of EIS data by means of a Nyquist and Bode plot.

Both Nyquist and Bode plots offer specific advantages. The complex plane is more frequently used for mechanistic analysis because often the number of relaxations and the nature of diffusion processes (e.g. planar diffusion and on side porous diffusion) are shown. On the other side, the Bode plane uses directly the frequency

as an independent variable, so that comparison between experimental and calculated data can be easier made .

The impedance of an electrode/electrolyte interface can be simulated by the equivalent circuit shown in fig. 3, in which R_e , C_{dl} , R_{ct} , Z_f represent respectively, the electrolyte resistance, the electrochemical double layer capacitance, the charge transfer resistance and the faradic impedance.

The total impedance, $Z(j\omega)$, can be written as:

$$(21) \quad Z(j\omega) = R_e + Z_f(j\omega) / [1 + j\omega C_{dl} Z_f(j\omega)]$$

From the previous equation we point out that for $\omega \rightarrow \infty$, the system impedance goes to the electrolyte resistance, therefore carrying out measurements at high frequencies, it is possible to calculate the electrolyte conductivity.

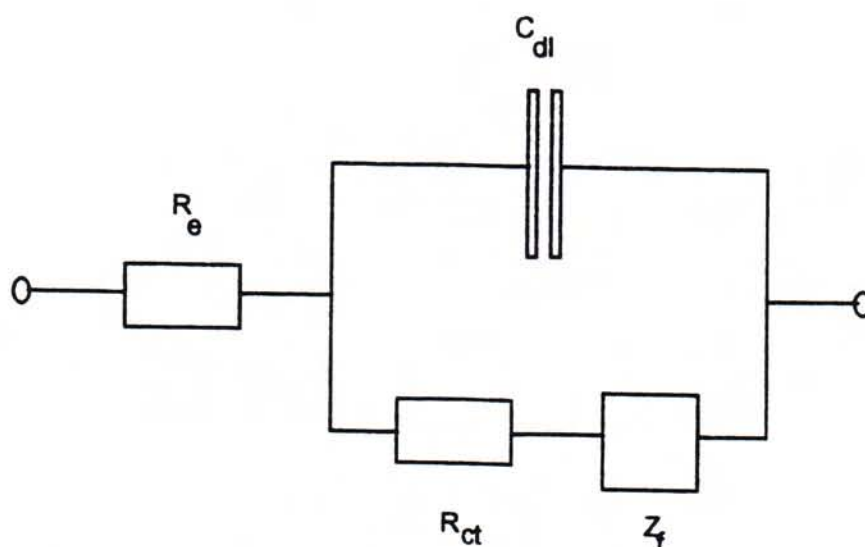


Fig. 3 - Equivalent electrical circuit of a generic electrode/electrolyte interface.

2.4 - Experimental set up.

The experimental instrumentation used to carry out the EIS measurements consist of a potentiostat-galvanostat (PG) Solartron mod. 1286 and a frequency response analyser (FRA) Solartron mod. 1250 (fig. 4), both controlled by a Hewlett Packard computer mod. 310. By means of transfer software [31] the EIS data were converted from HP BASIC to DOS format in a HP VECTRA mod. D1346A computer, upgraded

with a language processor card HP 82 300 B. The PG gives a d.c. polarisation on which the FRA overimposes an a.c. signal.

The FRA is constituted by a signal generator (SG) and by two analysers (AN). The SG superimposed to the d.c. polarisation, without phase shift, a perturbing sinusoidal signal, with a low amplitude and a changeable frequency. The AN receives, after an amplification, both the perturbing $S_p(t)$ and the response $S_r(t)$ signal from the system. Such a signals are sent to a correlator to be compared between them [19]. The correlation result gives, in a numeric form, the real (Z_{Re}) and imaginary (Z_{Im}) component of the impedance, making an integration of the signals over a time equal to an integer number of perturbing signal period (τ):

$$(22) \quad Z_{Re} = 1/\tau \int_0^{\tau} S_r(t) \sin \omega t \, dt$$

$$(23) \quad Z_{Im} = 1/\tau \int_0^{\tau} S_r(t) \cos \omega t \, dt$$

in which $S(t) = x_0 k(\omega) \sin[\omega t + \varphi(m)] + \sum A_m \sin(m\omega t - \varphi m) + n(t)$, is the sum of harmonics and parasitic noise. The integration is carried out to minimise the casual noise effect and increase the signal/noise ratio.

By integrating $S(t)$ we find that the only integral different from zero, is that of the first harmonic, while the other harmonics are rejected. In presence of a parasitic noise, the same result is obtained if the integration time is infinite. Really, τ can not be infinite, for practical reasons; therefore the signal/noise gain is correlated to the τ value. In practice for each frequency and defined τ value, we have a frequency band depending by τ .

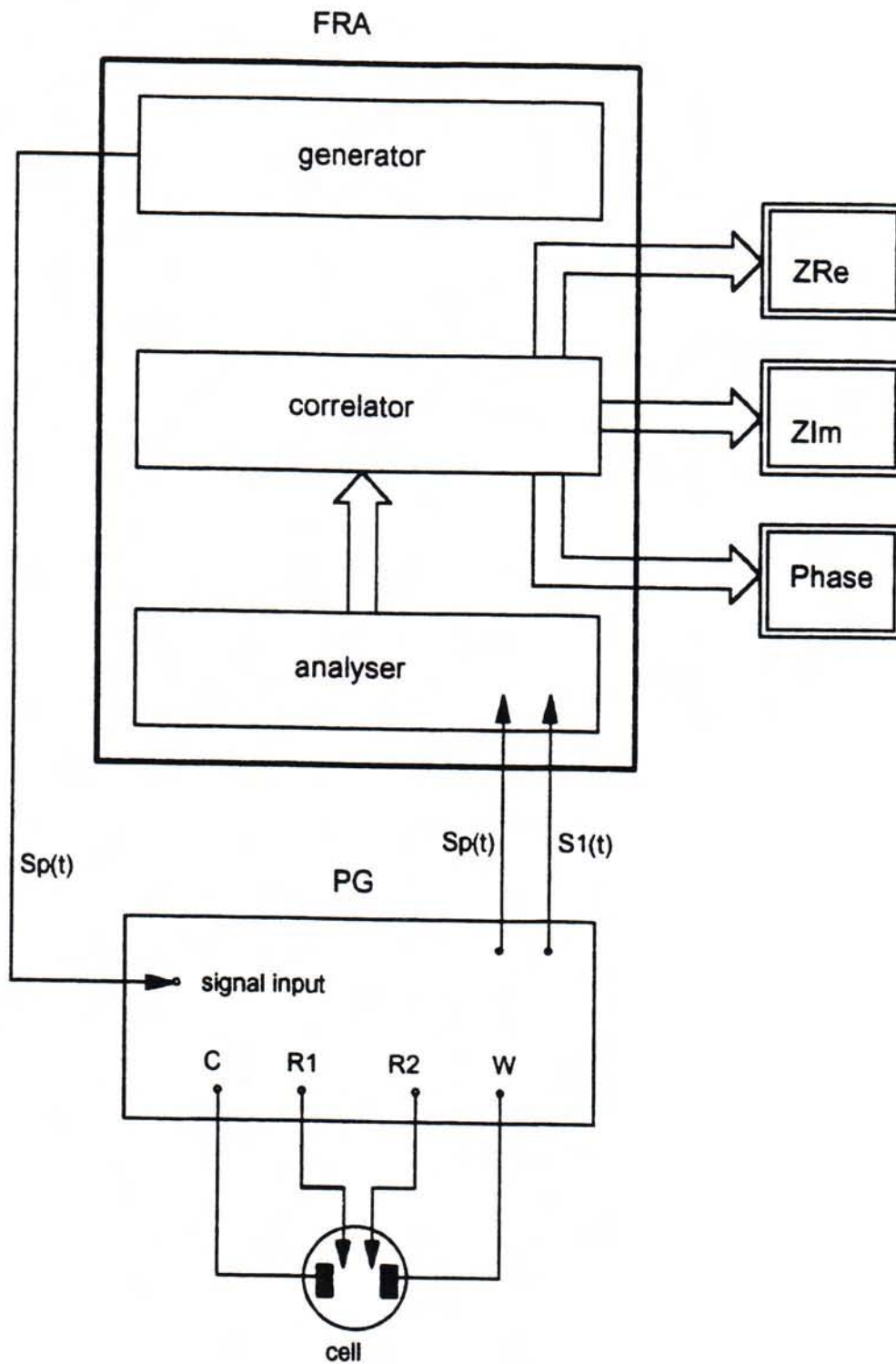


Fig.4 - Experimental instrumentation for EIS measurements.

The period τ is correlated to the frequency by:

$$(24) \quad 1/\tau = f \cdot 1/N$$

where N is the number of cycles of the examined signal.

The band width is then:

$$(25) \quad \Delta f = 1/\tau$$

The power of filtering the signal, suppressing the parasitic noise (higher order harmonic), is defined as the equivalent filter selectivity [14] and is expressed by:

$$(26) \quad \Delta f/f = 1/\tau f = 1/N$$

Finally, we can obtain the total impedance of the system under study:

$$(27) \quad Z(\omega) = \frac{\{\text{perturbation}\}}{\{\text{response}\}} e^{j\omega} = Z_{\text{Re}}(\omega) + j Z_{\text{Im}}(\omega)$$

3.5 - Measurement methodologies

The EIS measurements, using potentiostat-galvanostat (PG) and a frequency response analyser (FRA), can be carried out with three different electrodes configuration, as shown in fig. 5. The choice of a particular configuration depends on the information which we want to obtain.

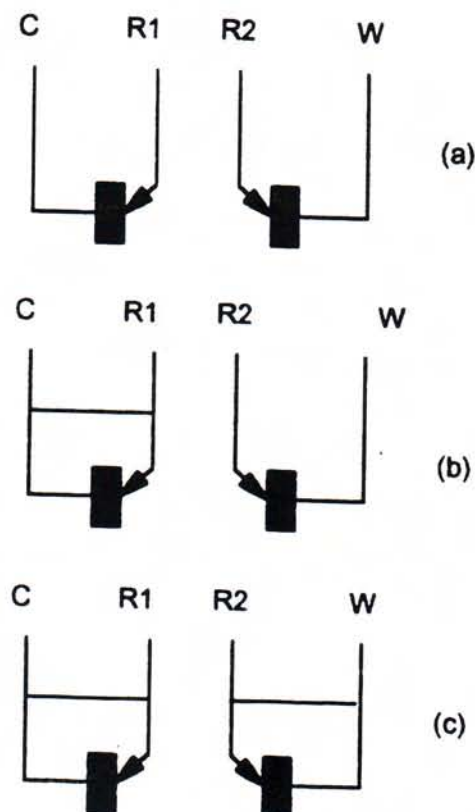


Fig. 5- Electrodes configuration that can be used to carry out EIS measurements (W= working electrode; C= counter electrode; R₁, R₂= reference electrode).

The four electrodes configuration allows to obtain information in the case of two electrodes separated by an active membrane (organic or inorganic).

If one want to study the interfacial phenomena of a single electrode, the fig. 5b configuration must be used, which allows a potentiostatic control of the working electrode or to measure the electrode potential during a galvanostatic polarisation.

If the aim of the measure is to examine the electrical conductivity of the electrolyte under study, the two electrodes configuration (fig 5c) is the suitable one. Such a configuration is the same used for the four contacts electrical resistance measurement. In fact this method allows to minimise the wire's resistance influence on the measured data; the current is applied throughout the counter and working electrodes, while the ohmic drop is measured between the two references electrodes connected to a very high impedance ($> G\Omega$) electrometer.

The measurements were carried out by applying a d.c. galvanostatic polarisation, with an superimposed sinusoidal signal ($236 \mu A/cm^2$ r.m.s.). The signal integration was made over 10 cycles, with 5 cycles of delay between two consecutive integration.

The choice of a galvanostatic polarisation come from the consideration that the traditional potentiostatic one does not allow to keep a null current if the open circuit voltage spontaneously changes with time.

On the contrary, in a galvanostatic operation, the electrode equilibrium will not be perturbed and the measurement result will correspond exactly to that in static conditions .

3.6 - Results of conductivity measurements.

The conductivity measurements were performed only after the system has reached the equilibrium condition, that is after the in situ cathode oxidation/lithiation process has had place [11].

A measure example is shown in fig. 6a as Nyquist plot, from which it is possible to extract the electrolyte resistance (R_e) by the high frequencies intersection on the real axis.

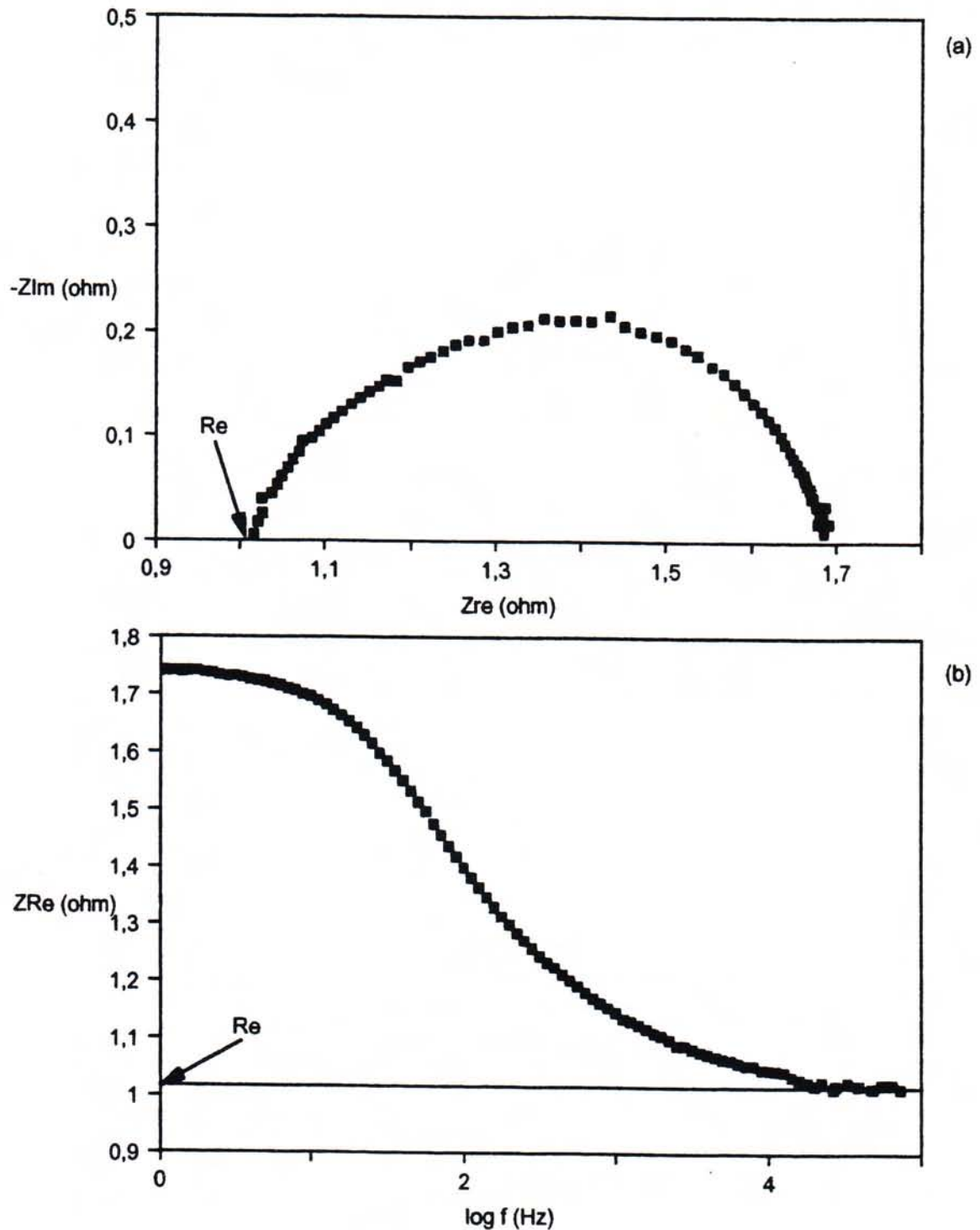


Fig.6 - Methodologies used to determine electrolyte electrical resistance by means of electrochemical impedance spectroscopy ($T=650^{\circ}\text{C}$, $p\text{O}_2=0.14\text{ atm}$, $p\text{CO}_2=0.30\text{ atm}$).

More precise results were obtained using a Z_{Re} vs. $\log f$ plot (fig. 7b). Such a plot is more useful because it shows a plateau at high frequencies from which it is very easy to draw out the electrolyte resistance and subtract the wire's inductive component of the impedance [30].

From the R_e measurement it is possible to determine the influence of mechanical load (L) applied by means of a dynamometer, through the current collector, on the anode/tile/cathode structure. The relationship between R_e value and the mechanical load is shown in fig.7.

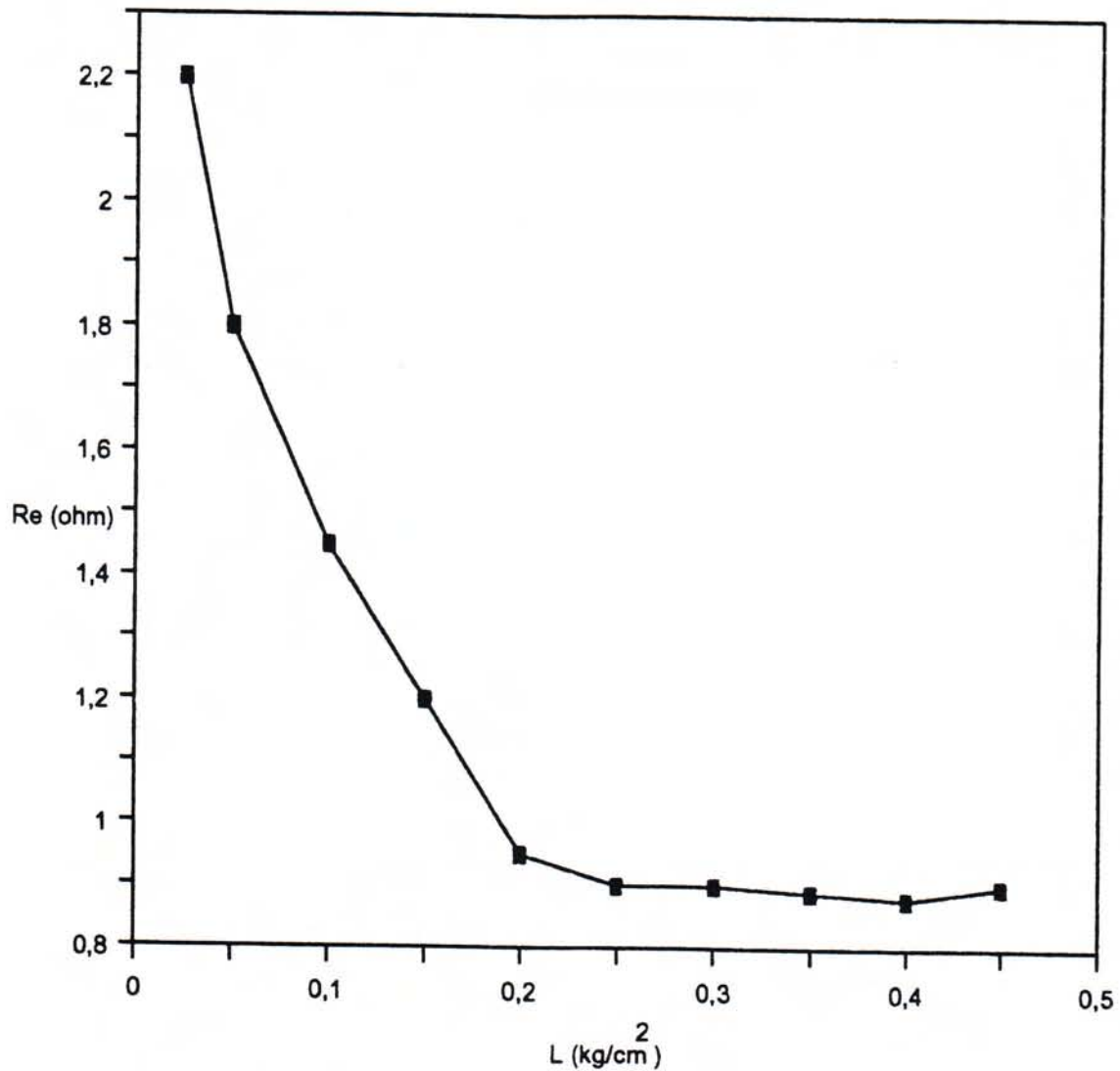


Fig.7 - Relationship between R_e and the mechanical load.

From the plot it is clear that an increase of L reduces the R_e value because the electrical contact between current collectors, electrodes and tile is improved. This effect is true up to 0.2 kg/cm²; after this value we could not obtain any advantage, on the contrary some mechanical troubles to electrodes and tiles could have place.

The main datum that can be calculated from the R_e value, is the specific conductance, expressed as S/cm. From this value, given the equivalent weight and the density of carbonate mixture, it is possible to calculate the equivalent conductance. Because we are studying a mixture of uni-valent carbonates, the equivalent weight is given by:

$$(28) \quad EW = \sum_i f_i (EW)_i$$

with f_i and $(EW)_i$ respectively, the molar fraction and the equivalent weight of the i -th component. Then the equivalent conductance is:

$$(29) \quad \Lambda = \sigma/d \sum_i f_i (EW)_i$$

The density (g/cm^3) of a carbonate mixture is temperature dependent in a linear way:

$$(30) \quad d_{\text{mix}} = a - bT$$

In the case of a lithium/potassium mixture (Li/K=62/38 %_{mol}) for the empirical equation in the range 500+700 °C, the coefficients values are $a = 2,353 \text{ g/cm}^3$ and $b = 4,532 \cdot 10^{-4} \text{ g/cm}^3/\text{°K}$ [8].

From a theoretical point of view, the mixture density should be calculated by the relationship $d_{\text{mix}} = \sum_i f_i d_i$. Such an equation gives an exact density value in the case in which there are no interactions between the solutes. In presence of carbonate mixture, a solvent in the classic meaning of the word, is not present: the solutes themselves behave as solvent. Therefore, the local interaction between the molten salts constituents are very strong and co-operative equilibrium are acting, with the generation of micro and macro complexes. Then, it is more useful to use the empirical eq. (30) with its errors, instead of the generic relationship which does not account for the components interactions.

The use of Λ instead of σ , is particularly useful in the case of molten carbonate mixtures. In fact, as the composition is changing the deviation from linearity is enhanced. The use of Λ allows to eliminate such a deviations because it is a parameter corrected for the mixture equivalent weight.

3.7 - Dependency of conductance from temperature and activation energy.

With the aim to calculate the activation energy for the conduction processes, the electrolyte resistance was determined as a function of temperature on the range 500÷700 °C.

The specific conductance increases with temperature, as we can expect for an ionic conductor, but not in a linear way (fig.8).

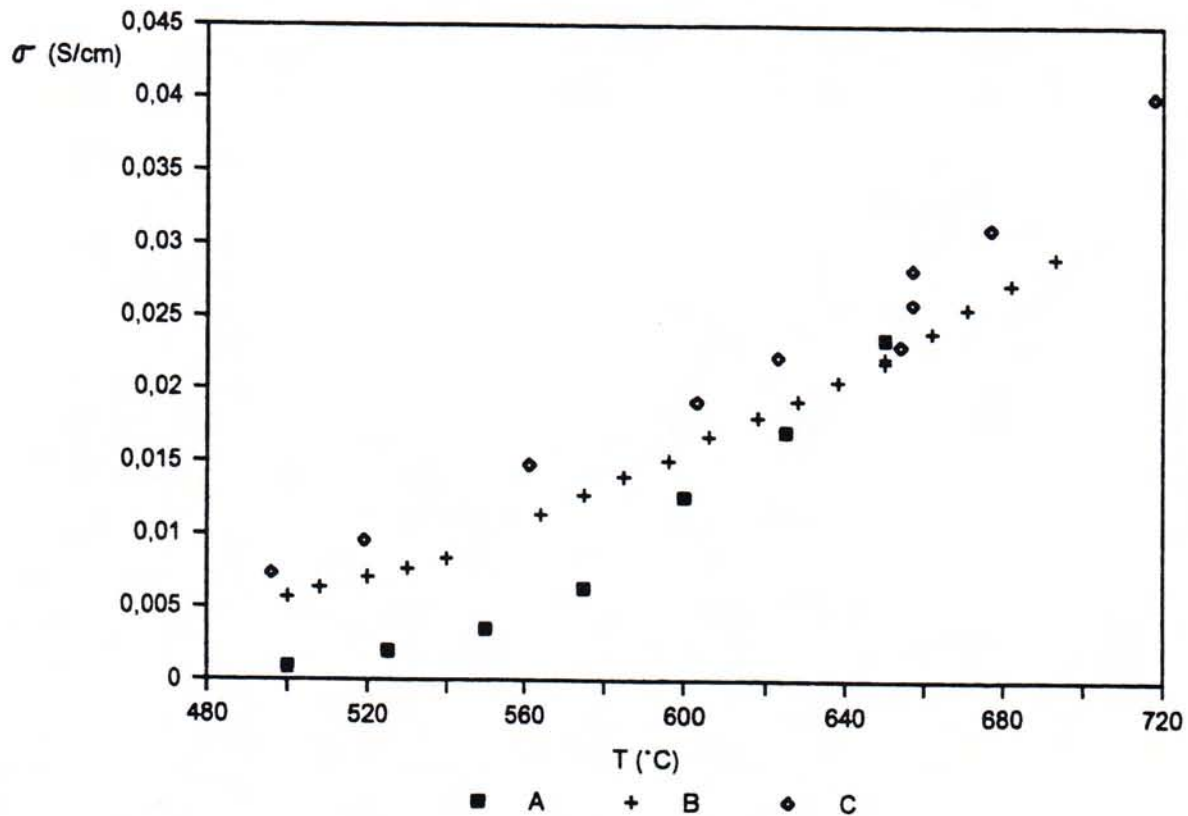


Fig.8 - Dependency of specific conductance from temperature.

The relationship between σ and T was analysed with the following equations:

$$(31a) \quad \sigma = a + bT$$

$$(31b) \quad \sigma = a + bT^2$$

$$(31c) \quad \ln \sigma = a + b/T$$

$$(31d) \quad \ln \sigma T = a + b/T$$

$$(31e) \quad \ln \Lambda = a + b/T$$

$$(31f) \quad \ln \Lambda T = a + b/T$$

The results of linear regressions relative to the previous equations, are summarised in tab.6.

Tab.6 - Specific and equivalent conductivity as a function of temperature.

Sample	Equation	a	err. a (%)	b	err. b (%)	r ²	E _{act} (kJ/mol)
A	$\sigma=a+bT$	-0.079	-3.09	1.54 10 ⁻⁴	12.03	0.9325	130±5 137±5 132±5 139±5
	$\sigma=a+bT^2$	-0.035	-6.03	1.34 10 ⁻⁷	10.37	0.9495	
	$\ln\sigma=a+b/T$	13.39	0.92	-15669.3	-4.22	0.9912	
	$\ln\sigma T=a+b/T$	21.13	0.57	-16512.8	-3.96	0.9922	
	$\ln\Lambda=a+b/T$	17.60	0.69	-15833.4	-4.16	0.9914	
	$\ln\Lambda T=a+b/T$	25.34	0.48	-16676.9	-3.90	0.9924	
B	$\sigma=a+bT$	-0.057	-1.37	1.22 10 ⁻⁴	2.47	0.9897	53±1 60±1 55±1 62±1
	$\sigma=a+bT^2$	-0.021	-2.28	1.02 10 ⁻⁷	1.52	0.9961	
	$\ln\sigma=a+b/T$	3.12	1.18	-6383.8	-1.66	0.9954	
	$\ln\sigma T=a+b/T$	10.88	0.32	-7245.3	-1.39	0.9967	
	$\ln\Lambda=a+b/T$	7.34	0.49	-6555.9	-1.58	0.9958	
	$\ln\Lambda T=a+b/T$	15.10	0.23	-7117.4	-1.33	0.9970	
C	$\sigma=a+bT$	-0.062	-3.79	1.36 10 ⁻⁴	8.09	0.9509	46±2 53±2 48±2 55±2
	$\sigma=a+bT^2$	-0.022	-8.95	1.14 10 ⁻⁷	6.71	0.9653	
	$\ln\sigma=a+b/T$	2.37	2.85	-5565.7	-4.26	0.9857	
	$\ln\sigma T=a+b/T$	10.14	0.66	-6431.2	-3.66	0.9894	
	$\ln\Lambda=a+b/T$	6.45	1.04	-5739.8	-4.12	0.9866	
	$\ln\Lambda T=a+b/T$	14.22	0.47	-6605.3	-3.56	0.9900	

In the table are shown the values of a and b coefficients, their relative errors, the correlation coefficient and, when it is possible, the activation energy following the general Arrhenius equation:

$$(32) \quad A = B \exp(-E_{act}/RT)$$

From the results of linear regression it is clear that the best correlation are found using the logarithmic form equations ($r^2 > 0,99$). The logarithmic expressions show the higher value for r^2 and the lower one for err. a and err. b.

Such a considerations let us to exclude the linear relationship, while confirm the presence of a thermal activated phenomena following the Arrhenius law (fig. 9).

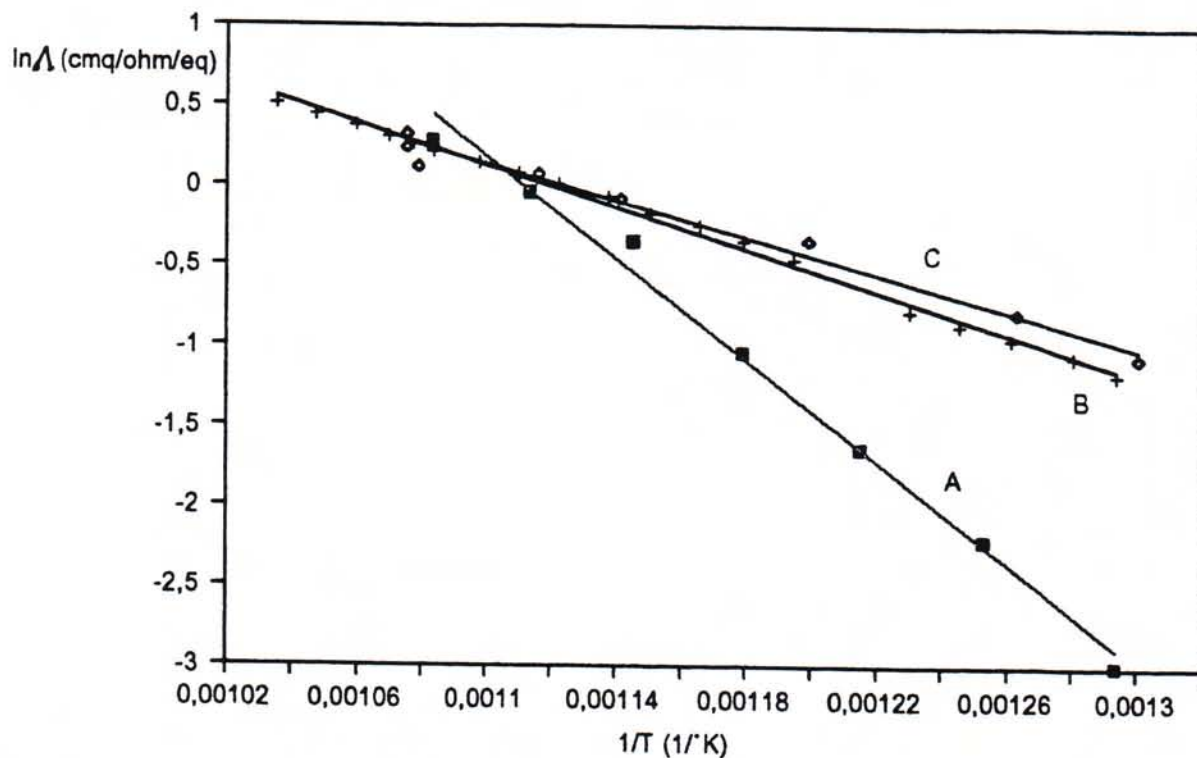


Fig.9. - Arrhenius plot for the equivalent conductivity of the tiles under study.

Generally, for a ionic liquid, the conductance Arrhenius relationship follows the eq. (7b). This equation is valid for not condensed systems; in our case the eq.(7a) relates in a better way the experimental data. That means the electrical conduction phenomenon is not a simple material transport controlled by diffusion/migration, but it involves jumps in empty spaces inside the liquid structure. The existence of such a free volume, could be not true, but a consequence of the not conductive γ -LiAlO₂ presence, which can simulate an empty space region.

The free volume law, could also be an evidence for the existence of complex compounds (clusters) [1], which form aggregates and as a consequence, the system is not longer purely condensed.

That last hypothesis, in agreement with the consideration that the molten carbonates are made by alkali metal ions and oxo-anions with six electronic lone pair per ion, could be confirmed by measurements in molten salts without ceramic matrix.

The literature data on Li/K carbonates mixtures, have been always correlated to the Arrhenius relationship for not condensed system, but the measurements were

carried out without $\gamma\text{-LiAlO}_2$. Only in a few cases the data are relative to tiles, but the authors did not try to use the equation for condensed systems.

3.9 - Influence of cathodic gas composition on electrical conductivity.

The molten carbonate fuel cell are fed with gas mixtures, with different composition for anode and cathode, with the aim to realise at electrodes/electrolyte interface the electrochemical reactions which will produce electrical current. Gas composition can be changed to optimise the cell performance, therefore its influence on tile conductance was investigated.

To avoid too much complicate response it was chosen to operate with tile C (tab. 3), in which the only gas mixture used was the cathodic one (O_2/CO_2). This choice was supported by the fact that the anodic gas ($\sim 70\% \text{H}_2$) should not influence the electrolyte composition. On the contrary, the cathodic gas, after solubilisation in molten carbonates, participates to acid- base equilibrium in the melt [25,26]:



The species O^{2-} , O_2^{2-} and O_2^- , if in sufficient concentration, could change the molten carbonate electrical conductivity. The concentration of oxide species is a function of $p\text{CO}_2$, therefore the measurements were carried out keeping constant the $p\text{O}_2$ (0,14 atm) and changing the $p\text{CO}_2$ (0,1 ÷ 0,5 atm). The results of these measurements are summarised in table 7.

From these results it is possible to point out that there is no correlation between conductivity and $p\text{CO}_2$. Such a result means that the concentration of the electrical active species (O^- , O^{2-} , O_2^{2-}) are very low and then, also if they have a lower steric hindrance and a higher mobility than CO_3^{2-} , they do not greatly influence the electrolyte conductivity.

The results agree with Selman data [27] on to the concentration of oxide compounds in molten carbonates. It is interesting to note that Selman data were

obtained in a completely different way, that is from relaxation measurements of electrode potential.

Tab. 7 - Arrhenius equation parameters as a function of carbon dioxide partial pressure (C sample, T=650 °C, pO₂= 0.14 atm).

pCO ₂ (atm)	Equation	a	err. a (%)	b	err. b (%)	r ²	E _{act} (kJ/mol)
0.1	$\sigma=a+bT$	-0.080	-3.09	1.73 10 ⁻⁴	9.19	0.9751	38±2 45±2 40±2 47±2
	$\sigma=a+bT^2$	-1.22	-8.52	7.10 10 ⁻⁶	7.59	0.9830	
	$\ln\sigma=a+b/T$	1.63	3.68	-4587.3	-6.15	0.9888	
	$\ln\sigma T=a+b/T$	9.42	0.64	-5470.9	-5.10	0.9922	
	$\ln\Lambda=a+b/T$	5.72	0.97	-4769.5	-5.89	0.9897	
	$\ln\Lambda T=a+b/T$	13.51	0.41	-5653.1	-4.92	0.9928	
0.2	$\sigma=a+bT$	-0.077	-2.81	1.75 10 ⁻⁴	7.94	0.9813	39±2 46±2 40±2 48±2
	$\sigma=a+bT^2$	-1.25	-7.11	4.63 10 ⁻⁷	6.45	0.9877	
	$\ln\sigma=a+b/T$	1.75	2.69	-4688.1	-5.91	0.9896	
	$\ln\sigma T=a+b/T$	9.54	0.56	-5571.7	-4.86	0.9930	
	$\ln\Lambda=a+b/T$	5.84	0.93	-4870.3	-5.63	0.9906	
	$\ln\Lambda T=a+b/T$	13.62	0.39	-5753.9	-4.67	0.9935	
0.3	$\sigma=a+bT$	-0.072	-2.67	1.66 10 ⁻⁴	7.47	0.9836	37±2 45±2 39±2 46±2
	$\sigma=a+bT^2$	-1.13	-6.81	6.83 10 ⁻⁶	5.87	0.9898	
	$\ln\sigma=a+b/T$	1.50	2.94	-4470.8	-5.00	0.9925	
	$\ln\sigma T=a+b/T$	9.28	0.47	-5354.4	-4.11	0.9949	
	$\ln\Lambda=a+b/T$	5.58	0.78	-4652.9	-4.77	0.9932	
	$\ln\Lambda T=a+b/T$	13.37	0.32	-5536.6	-3.96	0.9953	
0.4	$\sigma=a+bT$	-0.074	-2.91	1.70 10 ⁻⁴	8.18	0.9803	38±2 45±2 39±2 47±2
	$\sigma=a+bT^2$	-1.18	-7.36	6.97 10 ⁻⁷	6.48	0.9875	
	$\ln\sigma=a+b/T$	1.56	2.89	-4523.6	-5.05	0.9924	
	$\ln\sigma T=a+b/T$	9.35	0.48	-5407.3	-4.20	0.9947	
	$\ln\Lambda=a+b/T$	5.65	0.79	-4705.0	-4.84	0.9930	
	$\ln\Lambda T=a+b/T$	13.43	0.33	-5589.5	-4.06	0.9951	
0.5	$\sigma=a+bT$	-0.077	-3.27	1.75 10 ⁻⁴	9.31	0.9748	38±2 46±2 40±2 47±2
	$\sigma=a+bT^2$	-1.25	-0.82	7.20 10 ⁻⁶	7.47	0.9836	
	$\ln\sigma=a+b/T$	1.66	2.88	-4604.5	-5.26	0.9918	
	$\ln\sigma T=a+b/T$	9.44	0.51	-5488.2	-4.44	0.9941	
	$\ln\Lambda=a+b/T$	5.74	0.83	-4786.7	-5.07	0.9923	
	$\ln\Lambda T=a+b/T$	13.53	0.36	-5670.4	-4.31	0.9944	

4 - CONCLUSIONS

The calculated activation energy values, from specific conductance data, are consistent with that reported in literature [3, 4, 6, 7].

We have to notice that the only literature data determined on MCFC are those obtained by Vossen [20] ($E_{act} = 28 \pm 2$ kJ/mole), using the same cell of the present work, but with a different carbonate mixture ($\text{Na}_2\text{CO}_3/\text{K}_2\text{CO}_3 = 55/45$ % mol).

The activation energies by other authors were obtained working in carbonate mixtures without $\gamma\text{-LiAlO}_2$ and with not porous gold [6] or gold-palladium [7] electrodes.

Glugla [28] used tiles ($\text{Li/K} = 62/38$ %mol, $\gamma\text{-LiAlO}_2 = 45$ %w), prepared with the same methodology used in the present work, but with gold sputtered on (~ 3000 Å). Tanase [32] measured the resistance of the electrolyte tile ($\text{Li/K} = 62/38$ %mol, $\gamma\text{-LiAlO}_2 = 40$ %w) with a four probe a.c. impedance technique. The sample were polished by SiC abrasive paper and then the surface was painted with gold paint. Therefore it is possible to make a comparison of the data for these materials (tab. 8).

Tab.8 - Comparison between activation energy values for specific conductivity, (C^* =sample C three months after cell start up).

Sample	f_{meas} (kHz)	Carbonates/Ceramic	E_{act} (kJ/mole)
B	>25	0.82	53 ± 1
C	>25	1.08	46 ± 2
C^*	>25	1.08	38 ± 2
Glugla [28]	18	1.22	33 ± 2
Tanase [32]	>25	1.50	25

From tab.8, it is possible to point out that the lower E_{act} values are obtained with the higher carbonates/ceramic ratio, by means of a linear relationship.

To explain such a behaviour we have to consider the tile structure: on the ceramic particles a carbonate layer is adsorbed on which the bulk salt is flowing. Therefore, an electrolyte portion is immobilised by LiAlO_2 , another one is slowed down and, as a consequence, a reduced ions migration velocity towards the electrodes occurs.

It seems that to improve the electrical tile characteristics, it is better to use a high carbonate concentration, taking into account the necessity to maintain a stable and mechanically resistant tile structure.

After about three months from the cell start up, the activation energy decreases by 8 kJ/mole; probably that is due to an electrolyte redistribution between tile and electrodes.

We have to notice that, to measure the true tile conductivity it is necessary to use a frequency as higher as possible to avoid errors. Usually, the measure is carried out by means of a multimeter working at 1 or 2 kHz; at these frequencies the error can be of 10%, as can be seen in fig.10.

REFERENCES

1. D.Inman, D.G. Lovering, "Electrochemistry in molten salts", in Comprehensive Treatise of Electrochemistry, ed. J.O'M. Bockris, B.E. Conway, E. Yeager, R.E. White, Vol. 5, Plenum Press, N.Y., 1982
2. L.F. Grantham, S.J. Yosim, in "Molten Salts", ed. G. Mamantov, p.409, Marcel Dekker, N.Y., 1969
3. G.J. Kanz, J. Electrochem. Soc., **108** (1961) 1052
4. A.T. Ward. G.J. Kanz, Electrochimica Acta, **10** (1965) 849
5. S.V. Karpachev, G.V. Varab'ev, in "Electrochemistry of Molten and Solid Electrolytes", ed. M.V. Smirnov, Vol.1, Consultant Bureau, N.Y., 1961
6. Spedding, J. Electrochem.Soc., **120** (1973) 1049
7. Y.Miyazaki,M. Yanagida, K. Tanimoto,T. Kodama,S. Tanase, J. Electrochem. Soc., **133** (1986) 1402
8. Selman, H.C. Maru, "Physical Chemistry and Electrochemistry of Alkali carbonate Melts", in Advances in Molten Salt Chemistry, Vol.4, 1981
9. R.H. Perry, C.M. Chilton, "Chemical Engineers' Handbook", 5-th edition, McGraw-Hill, N.Y., 1975
10. L. Giorgi, "Allestimento di un laboratorio per la sperimentazione di celle a combustibile a carbonati fusi", ENEA Security Report, FARE/ICHI/ELC, July 1989
11. L. Giorgi, E. Simonetti, "Caratterizzazione di una cella a combustibile a carbonati fusi: tecnologie per la determinazione delle caratteristiche elettriche e risultati sperimentali", ENEA Technical Report, RT/ENERG/91/04.
12. G.D. Robbins, J. Branstein, in "Molten Salts", ed. G. Mamantov, p.445, Marcel Dekker, N.Y., 1969
13. D.D. Mcdonald, M.C.M. McKrube, "Electrochemical Impedance Techniques in Corrosion Science", Electrochemical Corrosion Testing, STP272, ASTM, 1981
14. C. Gabrielli, "Identification of Electrochemical Processes by Frequency Response Analysis", Solartron Technical Report, 1980
15. Gabrielli, "Use and Application of Electrochemical Impedance Techniques", Solartron Technical Report, 1990

16. Goldman, "Transformation Calculus and Electrical Transients", Prentice Hall Inc., N.Y., 1950
17. J.R. McDonald, M.K. Brachman, Rev. Mod. Phys., **28** (1956) 393
18. D.D. McDonald, Corrosion, **6** (1990) 229
19. C. Gabrielli, "Identification of Electrochemical Processes by frequency Response Analysis", Solartron Technical Report, 1980
20. J.P.T. Vossen, M. Sc. Thesis, Delft University of Technology, January 1989
21. G.D. Robbins, J. Branstein, in "Molten Salts", ed. G. Mamantov, p.470, Marcel Dekker, N.Y., 1969
22. H. Bloom, "The Chemistry of Molten Salts", p.81, Benjamin Inc., N.Y., 1967
23. L. Giorgi, E. Simonetti, G. Gavelli, NATO-ASI "Electrified Interfaces in Physics, Chemistry and Biology", p.16, July 23 + August 3, 1990, Varenna (Italy)
24. E.C. Subbarao, "Solid Electrolytes and Their Applications", Plenum Press, N.Y., 1980
25. M.L. Orfield, D.A. Shores, J. Electrochem. Soc., **135** (1988) 1662
26. L. Giorgi, "Dissolution behaviour of materials for MCFC cathode", NEDO Technical Report, NEDO-P-9082, March 1991, Tokyo
27. Lu, J.R. Selman, J. Electrochem. Soc., **137** (1990) 1125
28. P.G. Glugla, V.J. De Carlo, J. Electrochem. Soc., **129** (1982) 1745
29. A. Pozio, Thesis, University of Rome "La Sapienza", December 1991
30. L. Giorgi, E. Simonetti, A. Pozio, Fuel Cell Seminar 1992, p. 554, November 29 - December 2, 1992, Tucson (USA)
31. M. Stefanoni, ENEA, unpublished work.
32. S. Tanase, Y. Miyazaki, M. Yanagida, K. Tanimoto, T. Kodama, Prog. in Batt. Solar Cells, **7** (1988) 389.

Riprodotta presso il Laboratorio tecnografico della Direzione Relazioni dell'Enea
Viale R. Margherita 125, 00198 Roma

